Journal of Crystal Growth 566–567 (2021) 126155

Contents lists available at ScienceDirect

Journal of Crystal Growth

journal homepage: www.elsevier.com/locate/jcrysgro

Computational fluid dynamics modeling of a new high-pressure chemical vapor deposition reactor design

Pedram Yousefian, Siddha Pimputkar *

Department of Materials Science and Engineering, Center for Photonics and Nanoelectronics, Lehigh University, Bethlehem, PA 18015, USA

ARTICLE INFO

Communicated by Lijun Liu

Keywords:
High-pressure CVD
HPS-CVD
Computational fluid dynamics
Thin-film synthesis
InN
Group III nitrides

ABSTRACT

The design of a new super-atmospheric pressure metal organic chemical vapor deposition (MOCVD) reactor with spatially separated source zones and rotating susceptor is proposed and analyzed using computational fluid dynamics (CFD) techniques to determine fluid transport phenomena and suitability for thin-film synthesis of group III nitrides. This High-Pressure Spatial Chemical Vapor Deposition (HPS-CVD) reactor is designed to permit high-temperature growth of high-indium content group III nitrides. This is made possible by increasing the partial pressure of nitrogen by up to two orders of magnitude in the system thereby increasing decomposition temperatures of the group III nitride thin film. The effects of rector design, chamber height, system pressure, inlet flow rate, and rotational speed are investigated and discussed. Flow instabilities arising from the heated and rotating susceptor traversing separate source zones are minimized. Growth rates of group III nitride materials synthesized in an HPS-CVD reactor are estimated to be enhanced by approximately a factor of 10 compared to an existing super-atmospheric MOCVD reactor due to improved reactor design thereby providing comparable growth rates to current atmospheric MOCVD systems.

1. Introduction

Development of thin-film growth processes has become an influential research area of the semiconductor industry as it permits extending our capabilities in material synthesis and associated development of novel and more efficient devices. Metal organic chemical vapor deposition (MOCVD), for example, is a commonly used technique to make electronic and opto-electronic devices, such as light-emitting diodes (LED), lasers, thin-film photovoltaic elements, high-power, high-frequency emitters, and high efficiency electrical power converters [1,2]. Further improvements of group-III-nitride-based devices could benefit from increased growth temperatures due to anticipated improvements in crystal quality, morphology and associated reduction in impurity concentrations and defects. Furthermore, significant incorporation of indium (In) into ternary or quaternary group III nitride systems ($Al_xGa_yIn_{1-x-y}N$) is of interest, though challenged due to the low decomposition temperature of InN (~560 °C at 1 atm of nitrogen) [3,4]. Incorporation of desired concentrations of In into group III-nitride films is currently achieved via a delicate balance of reducing the growth temperature while maintaining sufficient mobility of adatoms to incorporate without introducing significant defects. While this approach can lead to successful growth of films with up to 25% In in $In_{1-x}Ga_xN$ [5,6] or $Al_xIn_{1-x}N$ films lattice matched to GaN with an In content around 17% [7,8], higher In-content films are currently challenging to achieve. To improve upon the crystal quality of high In-content films, higher growth temperatures are needed, while to increase the In-content of a film the nitrogen activity needs to be increased to raise the decomposition temperature of these group III nitrides [9]. This can be achieved by increasing the partial pressure of nitrogen-containing molecules during the growth of group III nitrides using MOCVD.

Studies on the elevated pressure growth of group III nitrides using MOCVD are sparse yet an experimental study demonstrated that the In-content can be increased by raising the nitrogen pressure of the system [10]. Extrapolation of the observed linear relationship between an increase in pressure and associated increase in In-content suggests InN can be grown at ~1000 °C for a system pressure of ~ 70 atm. They also showed that stable growth of the high In-content with $x < 0.65$ in $In_{1-x}Ga_xN$ is possible.

Literature reports on the existence of a super-atmospheric horizontal MOCVD reactor which could mechanically withstand pressures up to 120 atm [11–14]. Fluid dynamics in this system design, however, limits the processing window to a pressure range of 1–15 atm. This ultimately

* Corresponding author.
E-mail address: siddha@lehigh.edu (S. Pimputkar).

https://doi.org/10.1016/j.jcrysgro.2021.126155
Received 16 November 2020; Received in revised form 20 March 2021; Accepted 15 April 2021
Available online 20 April 2021
0022-0248/© 2021 Elsevier B.V. All rights reserved.

led to a low gas flow rates, slow growth rates (~200 nm/h), and poor quality films [15]. A horizontal flow reactor design is fundamentally limited in achievable pressures while maintaining desired growth conditions due to fluid dynamic considerations [16,17]. A vertical reactor design with a rotating-susceptor chamber design, on the other hand, is better suited for high pressure operations due to better control over achieving a uniform boundary layer and laminar gas flow.

A notable challenge for MOCVD reactors operating at elevated pressures is the detrimental increase in gas-phase pre-reactions of the precursors. To overcome these challenges, a new CVD reactor design is proposed which will minimize the probability of precursor pre-reactions via spatial separation of the precursors, while providing desirable fluid dynamic conditions for controlled synthesis of thin films. Development of such a CVD reactor necessitates proper analysis of the fluid dynamics and mass transport aspects within the system as reaction chamber design heavily influences film quality, uniformity, and deposition rate [18]. Successful CVD reactor designs have the ability to achieve a stable and vortex-free flow pattern at optimal operating conditions yielding optimal deposition rates and uniformity [19–21]. Advanced computational fluid dynamics (CFD) modeling techniques have been used to design and optimize performance of CVD reactors [22–29]. Vertical CVD reactors incorporating a rotating disc have also been studied, both theoretically and experimentally, during the last two decades [30–40]. This study applies this knowledge towards the design and optimization of a new super-atmospheric, vertical MOCVD reactor with spatially separated precursor zones, which will be referred to as a High-Pressure Spatial CVD (HPS-CVD) reactor. This paper reports on the design and CFD-based optimization of an HPS-CVD reactor design while providing an analysis of anticipated thin film growth rates as compared to an existing super-atmospheric MOCVD.

2. Design of an HPS-CVD

The HPS-CVD design can be classified as a vertical CVD reactor with a rotating susceptor. Critical to the design is the physical separation of precursors into separate chambers and a rotating susceptor carrying a substrate sequentially through each chamber in a circular motion. A schematic of the circular process flattened into linear representation is provided in Fig. 1. This design approach minimizes pre-reactions of precursors and limits their interaction to the period of diffusion through the boundary layer common to all chambers. The boundary layer thickness is decoupled from the rotational speed of the susceptor via mechanical control of the size of the gap between the chamber wall and the rotating susceptor. Each chamber has a dedicated gas source supplying user-determined gas mixture containing group III elements, nitrogen-containing species, inert gases, or dopants precursors.

The basic approach to the proposed HPS-CVD is similar to existing spatial atomic layer deposition (SALD) approaches [41] in which precursors are either spatially or temporally separated and a substrate moves through different precursor zones. Important differences to the HPS-CVD include operation at higher temperatures and pressures while requiring mixing of two or more precursors from different precursor zones prior to deposition as reactions on the substrate are not surface-limited reactions as is the case for ALD. SALD specifically prevents mixing of precursors from different zones. Due to the lower pressure operations and ability to operate as an open system, roll-to-roll operations are possible for SALD whereas the HPS-CVD requires a sealed system to achieve super-atmospheric pressures necessitating circular motion of a substrate through the zones.

In general, CVD reactors exhibit different types of flow patterns, including spiral flow due to combined free and forced convection and laminar flow due to pure forced convection. These flow patterns are a result of the system pressure, fluid type and geometry of the system. To determine which flow mode is dominant, the dimensionless parameter Gr/Re^2 is commonly used. As the value of this ratio decreases, forced convection flow becomes more dominant, while when it increases free convection flow dominates [30]. While this approach works well for typical CVD reactors, due to the complexity of the HPS-CVD this value could not be reliably determined and hence the origin of observed flow dynamics was elucidated via changing certain parameters, such as changing substrate rotational speed or inlet velocity in a stagnation flow CVD reactor [30,42–44]. The interaction of some of these parameters along with the resulting gas flow conditions within the chamber and resulting estimated crystal growth rates are evaluated in the following sections.

Control of growth conditions is achieved via independent control of gas composition in each chamber, gas flow rates into each chamber, geometry of each chamber, geometry of the barrier between adjacent chambers, total system pressure, separation distance between barrier and susceptor, angular rotation speed of the susceptor and susceptor temperature. Most of these variables could be dynamically controlled during growth, while some may need to be controlled run-to-run. Proper selection of these variables will lead to optimal growth conditions which are in part characterized by laminar, vortex-free flow of gases into and out of the system.

3. Methods

Increasing the pressure within a CVD reactor leads to an enhancement of undesired phenomena including increased probability of turbulent flow formation and increased gas phase reactions. To manage such a tool, the mechanical and control systems also become more complex. CFD models are a crucial first step to develop a basic understanding of the transport phenomena in an HPS-CVD reactor design and can predict viability of the design before investing in prototyping the tool.

CFD simulations were performed using COMSOL Multiphysics® [45], which uses the above relationships as the basis for numerical calculations, while SOLIDWORKS® [46] was used to design 3D models of the system. After importing a SOLIDWORKS model into the COMSOL

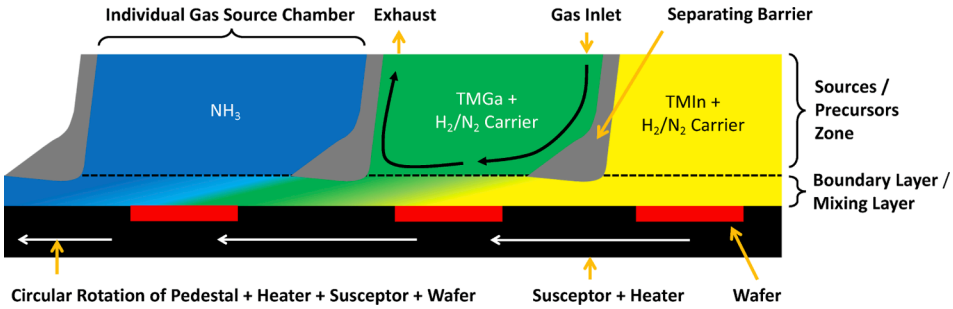

Fig. 1. Cross-section view of a flattened, partial arc of the HPS-CVD. A heated wafer traverses, via rotation of the susceptor, underneath each chamber sequentially picking up precursors provided in the chambers. Chambers are pressurized, pressure-balanced, and filled with common precursors for undoped $In_{1-x}Ga_xN$ growth. See Fig. 2 for a schematic of the HPS-CVD.

platform, an unstructured mesh with boundary layer mesh was applied. COMSOL allows coupling of heat transfer and fluid flow (K-ω model) physics in three dimensions. CFD simulations were performed by considering the following parameters: incompressible gas type, substrate temperature ($T_{substrate}$), uniform inlet flow velocity (V_{inlet}), angular velocity of rotating substrate (ω), and outlet pressure (P). The following boundary conditions were used for all the simulations:

- No slip boundary condition for all chamber walls.
- The velocity of inlets gas is limited with values.
- The outlets of reactor are specified as pressure outlet.
- The temperature of inlet gas is room temperature.
- The initial temperature values for all reactor walls are set to be at room temperature, while the temperature of wafers surface is set to be at 1393 K.

The impact of reactor design and related process parameters was performed by developing an initial design, analyzing it and developing a new major revision to address identified shortcomings, i.e. developing a new generation. In total, three generations were analyzed and will be reported on. The characteristics and evaluated parameters for each major design generation is summarized in Table 1.

For the first-generation HPS-CVD design, the analysis focused on the chamber design and gas inlet geometries and their relationship. The second-generation design proposes spiral shaped chambers with curved separation barriers while analyzing the effect of gas type, inlet flow velocity and reactor pressure. The third generation refines the system and minimizes gas recirculation and vortices formation at higher reactor pressure (100 atm) while analyzing the effect of inlet flow velocity and substrate rotational speeds.

4. Results and discussion

Outcomes of the various CFD modeling generations will be reported on in individual sections separated by the three major design generations.

4.1. First-generation design

The first-generation design was based on the introduction of gases from a horizontal plane into the camber from the sides while the exhaust was on top of each chamber. This design has the advantage of being able to tailor the gas inlet velocity profiles to each individual gas (or gas mixture) and its specific properties while ensuring laminar flow into the chamber. The system was composed of six equal sized closed pockets (chambers) of 1-inch height, which were bound by 0.5-inch thick separation barriers which provided 0.2-inch gap to the underlying susceptor. The 5.8-inch diameter susceptor carries four 2-inch diameter wafers about the central axis of the system (see Fig. 2).

Table 1
Characteristics and parameters evaluated using CFD for each of the three HPS-CVD design generations.

Design generation	Characteristics	Evaluated parameters
1st	- Introduce individual source gases separately into chamber - Horizontal inlets and vertical outlets	Inlet introductory angle Chamber height
2nd	- Swap inlet and outlet direction and position - Spiral shape curved separation barrier	Gas type (pure H_2 or N_2) Inlet flow rate (V_{inlet}: 0.01, 0.1, or 0.5 m/s) Outlet pressure (P: 1 or 100 atm)
3rd	- Circular Outlet outside - Reduce the thickness of separation barrier	Inlet flow rate (V_{inlet}: 0.05, 0.1, or 0.2 m/s) Substrate rotational speed (ω: 100, 200, or 400 rpm)

To study the basic performance of the design, initial CFD simulations were performed using pure hydrogen gas as the internal fluid at 1 atm. Hydrogen is the most favorable fluid to enable desired flow patterns due to its fluid properties, while nitrogen most readily leads to flow instabilities. To visualize mass transport, velocity streamlines, which represent the direction of a massless fluid element travels at any point in time, were chosen to represent collective flow of gases in the system.

The first-generation design led to desired laminar flow patterns within the gas inlet channels, though vortices appeared at the entrance region to the chamber, as presented in Fig. 3a, due to the required sharp transition in flow direction resulting in onset of turbulent flow. These vortices demonstrate flow pattern instabilities in the reactor, which could lead to substantial mixing of gases in the boundary layer with precursors in the chamber due to them being pulled into the chamber via turbulent flow leading to enhanced pre-reactions of the precursors and resulting nonuniform deposition on the substrate. A vortex-free flow pattern is necessary to reach maximum deposition rate and uniformity [20,21,47].

To minimize vortex generation due to gas-inlet effects, the introductory angle of the gas inlet channels was decreased from 90° to the circle tangent of the rotating susceptor (Fig. 2c). CFD simulation results show at an angle of 40° turbulent vortices generation as a result of gas introduction could be eliminated. Furthermore, gases introduced into one chamber communicated to the neighboring chamber (which was held at the same pressure) via mass transport in the boundary layer (Fig. 3b).

Upon removal of gas-inlet vortices, a second type of vortices were observed deeper within the chamber. To determine their origin, the effect of internal chamber height on turbulent vortex generation was investigated. As Fig. 3c shows, quantity and intensity of vortices were significantly and proportionally reduced via a reduction in chamber height, which is in agreement with literature studies in fluid dynamically comparable systems [42,48,49]. The primary origin of these vortices is due to buoyancy forces.

While laminar flow was achieved, the resulting small height difference between the substrate and roof of the chamber led to a significant increase in roof wall temperature (from 400 °C to 800 °C). An increase in wall temperature will result in a reduction of important material properties, such as strength and corrosion resistance reducing the selection of suitable materials. Moreover, separation barriers are placed within a very short distance (0.2 in.) to the susceptor where the barrier wall temperature reaches up to ~1000 °C. This is considered undesirable as it could lead to unwanted depositions on separation barriers' surfaces and as a result may disrupt the boundary layer pathway due to roughening and resulting possible disruption of laminar flow, along with increasing maintenance requirements.

Although the first-generation design demonstrated that the inlet gas could enter the chamber with a laminar flow pattern from the edge and communicate to the neighboring chamber via the boundary layer, it still suffered from turbulent flow within the chamber for reasonable chamber heights. Furthermore, analysis of the streamlines clearly suggested that the source gases would not evenly nor completely distribute over the wafer leading to non-uniform growth. The reason for this effect was determined to be a direct result of the gases fighting the outwards centrifugal force of the rotating susceptor.

4.2. Second- generation design

To overcome challenges identified in the previous design, the second-generation design introduces gases vertically from the top and closer to the central axis for each chamber. The centrifugal force of the rotating susceptor hence naturally guides the gases to the outer wall of the chamber where exhaust outlets are positioned. To further tailor gas flow, spiral shaped separation barriers were introduced to better guide

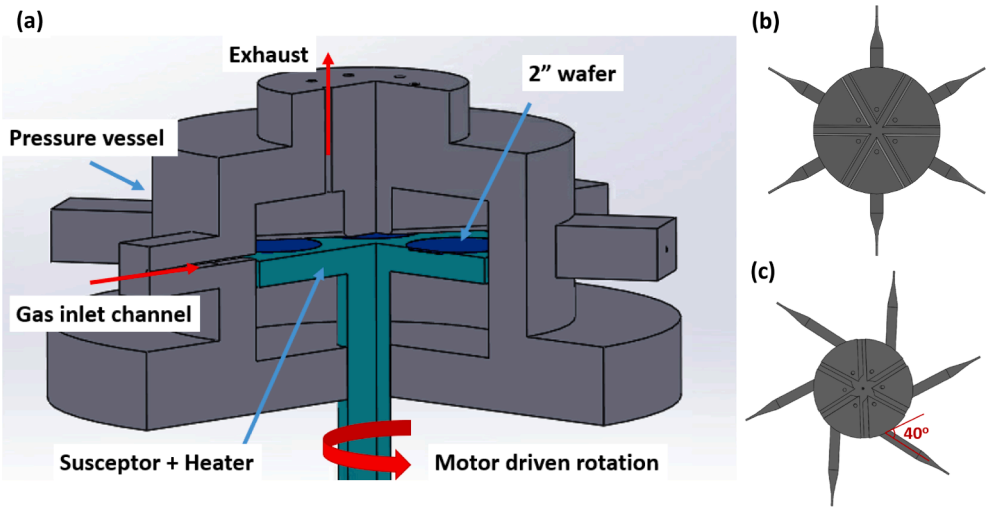

Fig. 2. a) Cut-away view of the SOLIDWORKS model of the first design of an HPS-CVD reactor including 6 chambers with 1-inch height. Each chamber has an individual gas inlets and outlets. Reactor is designed to be capable of growing four 2-inch wafer (shown in blue) sitting symmetrically on a rotating susceptor (shown in teal). Top view of gas cavity, which represents the gaseous volume within the design, with horizontal inlets (b) normal to the outer surface of the chamber and at (c) 40° angle with tangency line. (For interpretation of the references to color in this figure legend, the reader is referred to the web version of this article.)

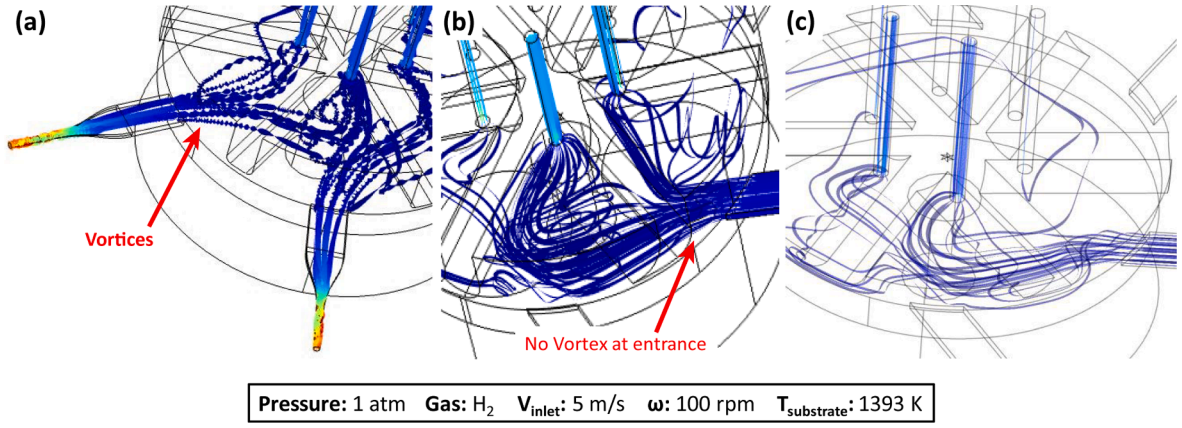

Fig. 3. a) Velocity streamlines of CFD modeling results of first reactor design, 6-inch chamber inner diameter, showing laminar flow pattern was achieved throughout the inlet, however, vortecis appeared as soon as source gas introduce to the chamber. b) Demonstrates the effect of reducing the gas inlet entrance angle to 40°. Vortices didn't appear at the entrance but a recirculation pattern can be identified. c) Represents the effect of decreasing internal chamber heights by factor of 3; recirculation patterns reduced significantly.

the source gas over the entire wafer surface, thereby preventing vortex formation due to sharp changes in inlet gas flow velocities, and have a similar exposure time. A 5°—10° draft was applied to the top of the chamber to continuously reduce the height of the chamber with increasing distance from the central axis. This ensures an approximately constant cross-sectional area, and hence gas volume, as a function of radius despite an increase in arc length within a chamber with increasing distance from the central axis. Unlike the first-generation design where chambers had a uniform distance separating each other along the arc (0.5 in.), the second-generation design the chambers distance increased from 0.2 to 1.65 in. with increasing radius. Moreover, the distance between susceptor and bottom of separation barriers was reduced to 0.1 in. to achieve a uniform boundary layer flow pattern.

Fig. 4 presents the optimized design for this generation of an HPS-CVD reactor. It includes six vertically tailored gas inlets and six horizontally exhaust outlets aligned with the tangent of the susceptor. A 5° draft was applied to the top surface of the chamber.

This reactor design was analyzed using two different pure gases: hydrogen (H_2) and nitrogen (N_2). These two gases are considered to be the two extreme cases for gas flow behavior in the system as trace concentrations of metal organics do not significantly impact fluid properties and ammonia has fluid properties which lie between pure H_2 and N_2 gases.

Fig. 5 compares the resulting fluid dynamic patterns for pure H_2 and N_2 gas in the system. It can be seen that nitrogen gas is more susceptible to formation of vortex patterns above laminar boundary layer. This was anticipated, as Giling [16] and Takahashi et al. [17] have already reported that nitrogen creates more unstable flow patterns compared to hydrogen in high flow rates for horizontal MOCVD reactor due to nitrogen having a lower thermal conductivity and higher viscosity as compared to hydrogen. These fluid properties lead to an easier onset of turbulence when the nitrogen gas reaches the hot susceptor and expands while moving slower due to its higher viscosity. All the while, the colder nitrogen will move faster leading to shear interactions and resulting vortex formation. While it is possible to change the ratio of nitrogen to hydrogen gas in the system to minimize vortex formation, this approach would limit the synthesis capabilities of the tool and is hence undesired.

Regarding fluid flow and wafer surface coverage, two different flow patterns were identified. The pure nitrogen carrier gas exited the system relatively quickly, whereas the pure hydrogen carrier gas was able to divert its flow and remain within the boundary layer for multiple rotations of the susceptor. This difference in behavior can be explained by looking to the significantly longer development period needed for nitrogen gas to develop into a fully developed velocity profile as compared to hydrogen, in part due to higher viscosity of nitrogen compared to hydrogen, making it in effect more sluggish [16]. While it would appear the nitrogen carrier gas could lead to more uniformity in the growing film given the single pass of the gases over the wafer during the initial

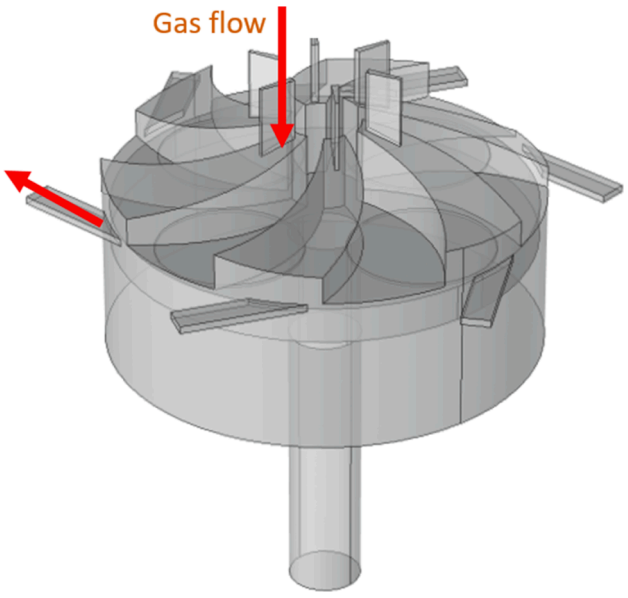

Fig. 4. Gas cavity of second-generation design of a HPS-CVD chamber with six spiral shape chambers with 5° draft on the top. Gases are introduced vertically from the top and closer to the central axis for each chamber. Individual exhausts are positioned horizontally.

introduction cycle, the impact of increased carrier gas entrapment in the boundary layer beyond the initial cycle requires further investigation.

The impact of inlet speed was studied to determine if conditions exist which provide laminar flow patterns within the system (Fig. 6). The study suggests there is an upper limit on acceptable gas inlet speed. Below this upper bound, vortices are negligible, though cannot be entirely eliminated. The observed vortices are weak and do not perturb the flow significantly, though they suggest memory effects could appear upon a change in precursor concentration within the inlet gas stream. This could lead poorly defined interfaces or imprecise alloy compositions.

While lower inlet velocities lead to a desired reduction in recirculation and vortices patterns, the ability for the gas to fully cover the wafer surface also decreases. As presented in Fig. 6a, even when laminar flow conditions exist, the source gas don't cover the entire surface of the substrate within the first cycle potentially leading to nonuniformities in the growing films. As such, a lower bound for the inlet gas speed exists. The optimal inlet gas flow speed for the HPS-CVD reactor is found to be around 0.1 m/s as presented in Fig. 6b.

To study the effect of pressure, flow patterns were studied at 1 atm and 100 atm system pressure (Fig. 7). While Fig. 6b demonstrated laminar flow patterns for the second-generation design for a chamber pressure of 1 atm, vortices appeared when increased to 100 atm. An important contributor to the onset of vortices formation was identified to be the perfectly vertical orientation of the separation barrier.

4.3. *Third-generation design*

To reduce vortex formation at higher pressures due to vertical chamber separation barriers, the third-generation tapered the barrier to improve fluid motion and gas transitions to the adjacent chamber via the boundary layer. The thickness of the separation barriers between the chambers was thinned as to reduce surface area for undesired reactions to occur. The inlet gas channel width was increased to cover the radius of chamber for better flow uniformity and tailored channels were discarded to simplify the manufacturing process. The susceptor diameter was reduced from 5.8 in. to 5.5 in. to increase the gap between the rotating susceptor and chamber walls to facilitate the exhaust gas flow. The exhaust was modified to become one common exhaust completely

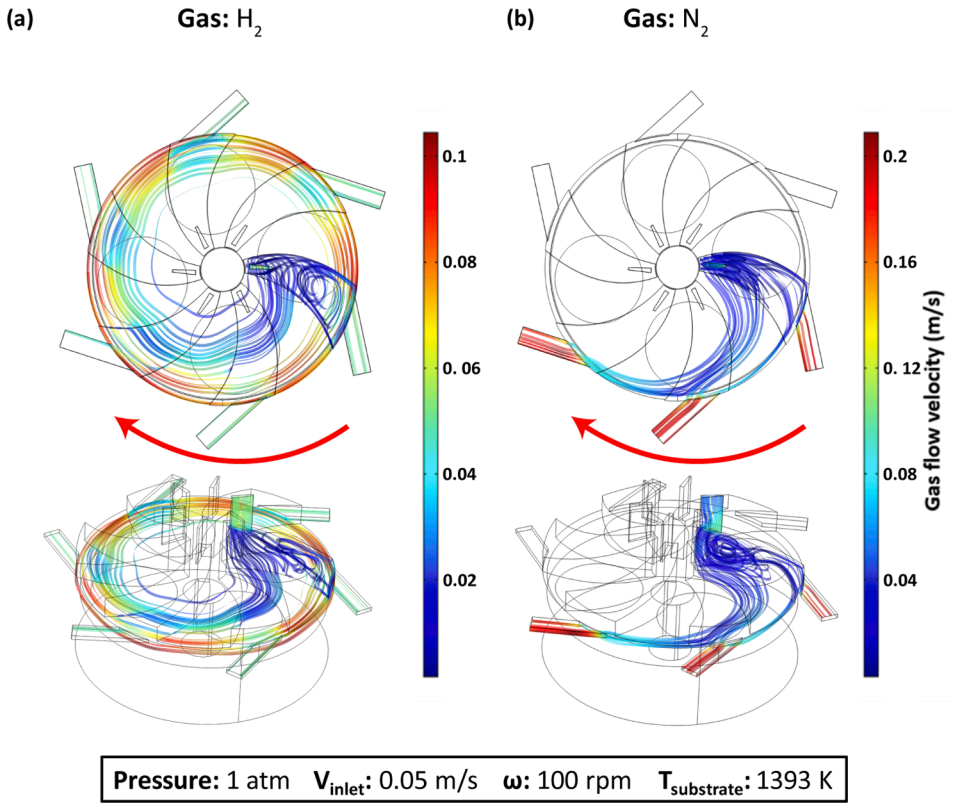

Fig. 5. Velocity streamlines from CFD modeling in second design generation are presented to demonstrate effect of gas type on flow for (a) pure hydrogen gas and (b) pure nitrogen gas.

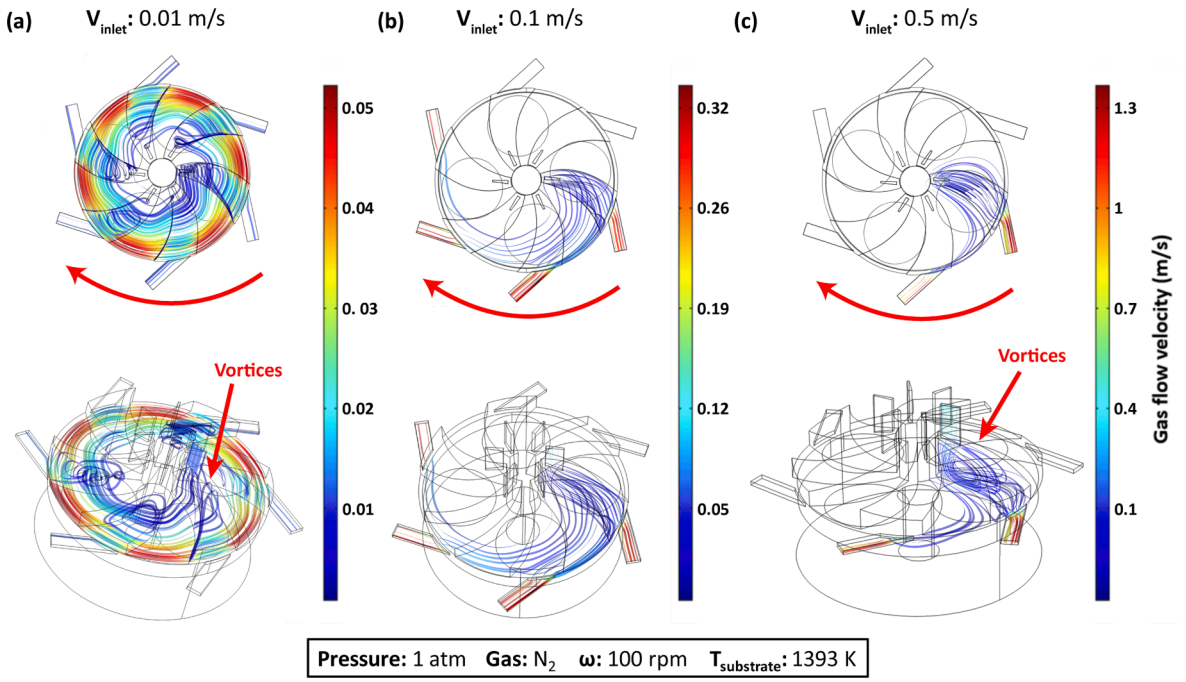

Fig. 6. Velocity streamlines in second-generation design demonstrate effect of inlet flow rate: a) Laminar flow pattern were observed but the inlet gas source didn't fully cover the substrate surface and takes a long time to leave the chamber. b) Optimized inlet speed to achieve laminar flow patterns which cover the whole substrate surface. c) Recirculation vortices re-appear with increased inlet speed.

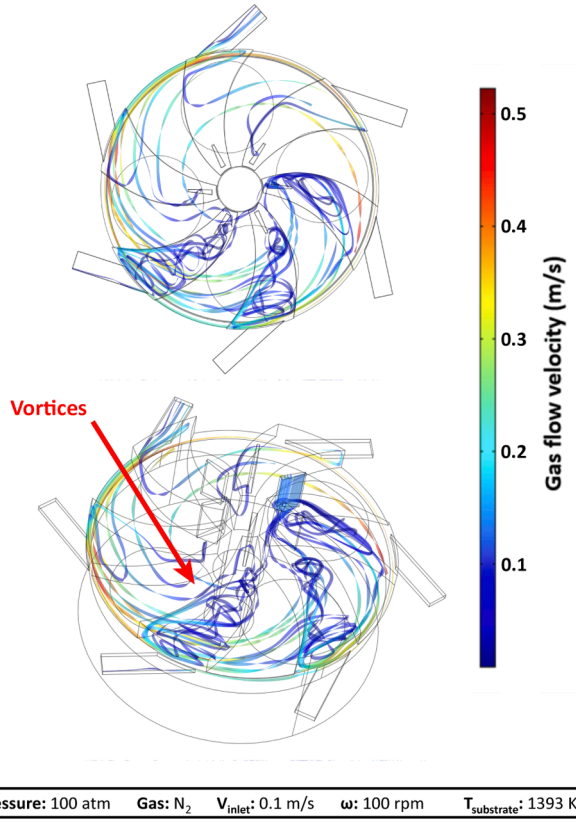

Fig. 7. Velocity streamlines for second-generation design demonstrate impact of reactor pressure. Vortices appear upon increasing system pressure.

encompassing the outer rim of the susceptor to minimize gas recirculation and improve flow pattern through the chamber. Fig. 8 depicts the gas cavity of this revised design.

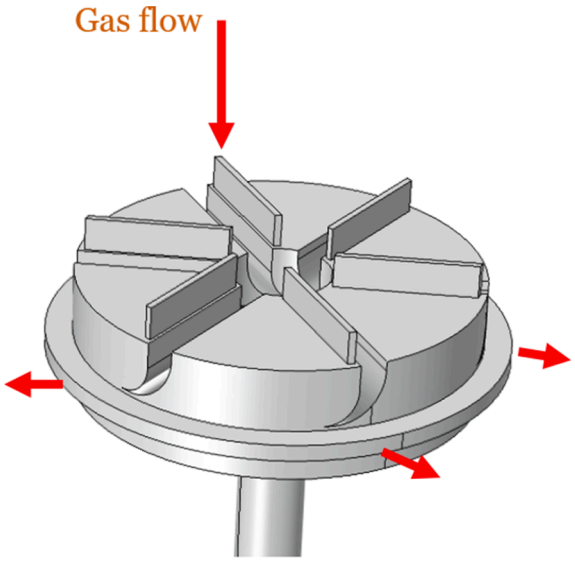

Fig. 8. Gas cavity of the third-generation design of HPS-CVD chamber with spiral shape chambers with a thinner barrier, which has 6 vertical inlets and one circular outlet outside.

Overall, CFD modeling studies demonstrated that gas recirculation and vortices reduced significantly compared to the second-generation design at 100 atm outlet pressure, as presented in Fig. 9.

The effect of rotational speed and inlet velocity on the flow pattern was investigated for this design to determine robustness of parameter space that can be accessed during growth. Nitrogen was used for all situations as it is known to be the most challenging gas for the system to provide stable flow conditions. Fig. 9 and Fig. 10 show gas flow patterns throughout the chamber when the rotational speed increases from 100 to 800 rpm and inlet velocity reduces from 0.1 to 0.04 m/s, respectively.

Simulation results suggest that for a specific rotational speed there is

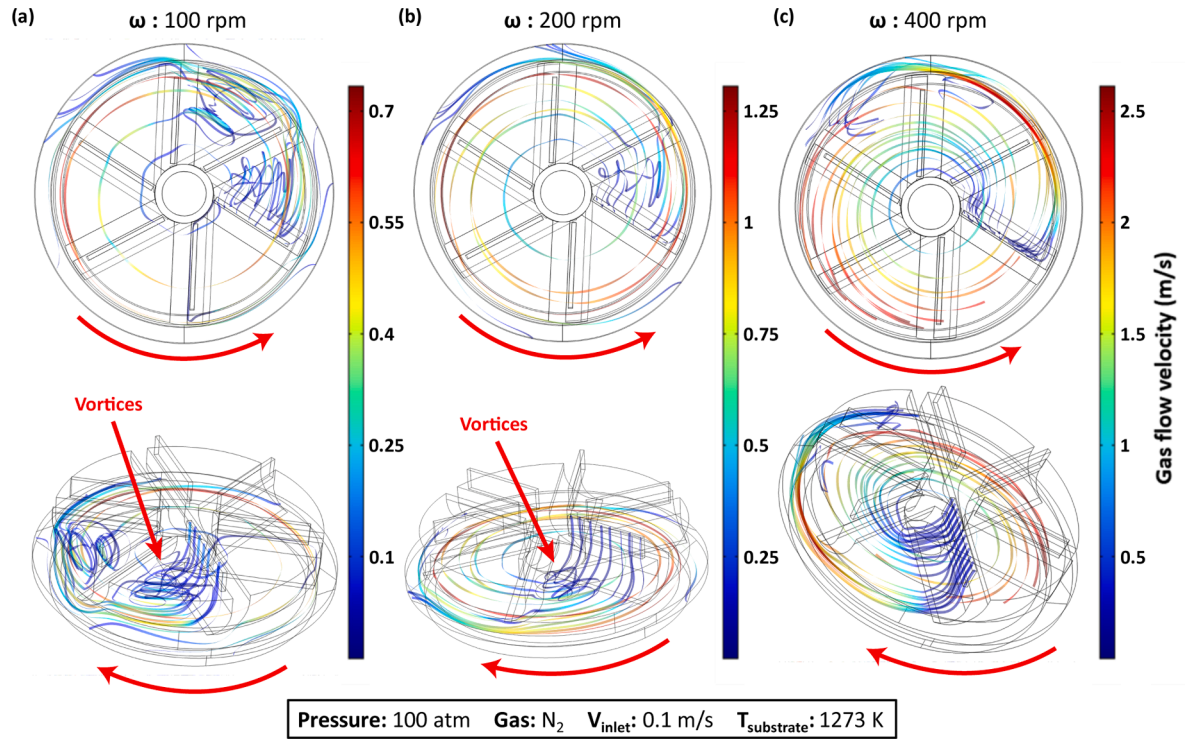

Fig. 9. Velocity streamlines for third-generation design demonstrate effect of rotational speed of susceptor rotating at a) 100 rpm, b) 200 rpm, and c) 400 rpm.

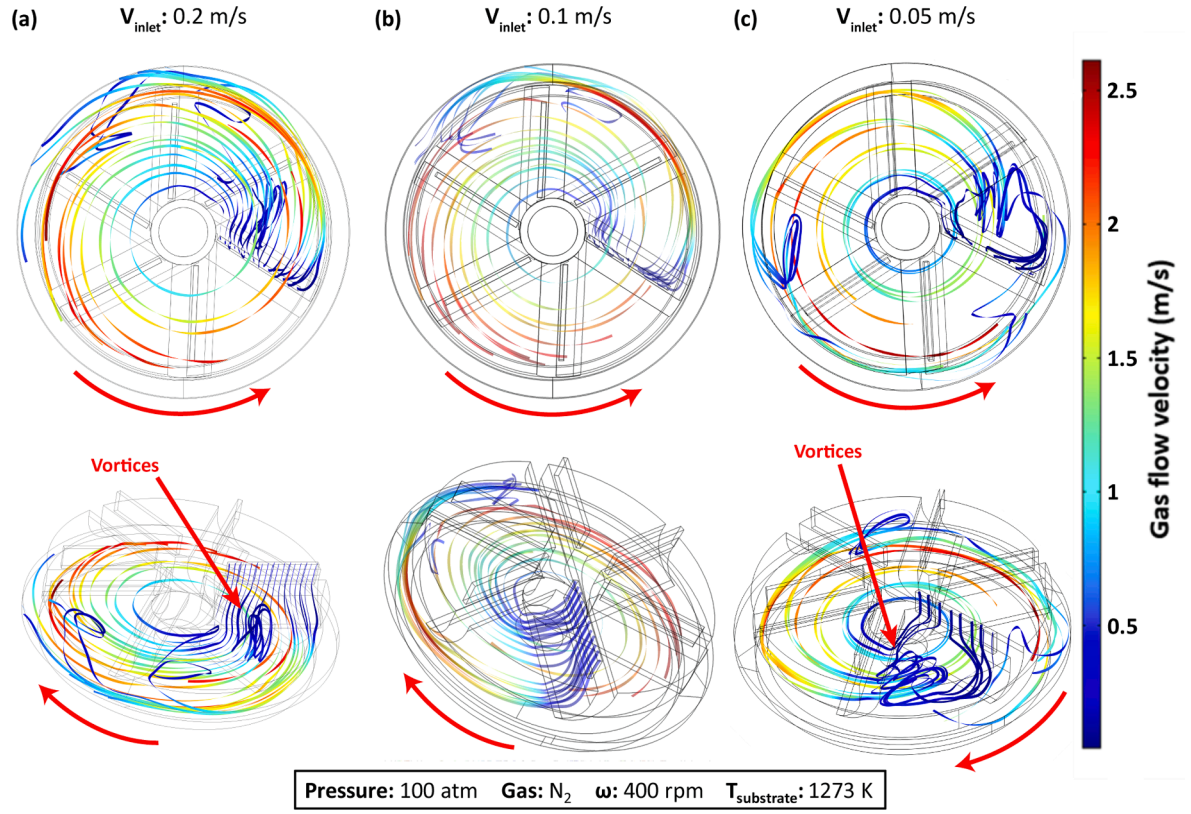

Fig. 10. Velocity streamlines for the Third-generation design demonstrating effect of inlet gas flow velocity at a) 0.2 m/s, b) 0.1 m/s, and c) 0.05 m/s (velocity color scale is identical for all).

an associated optimum inlet velocity. This occurs when the inlet gas speed as it approaches the susceptor closely matches the average linear velocity of the rotating disk. At a certain deviation from the speed matching condition, either via susceptor rotational speed reduction at constant inlet velocity or decreasing inlet velocity at constant susceptor rotational speed, vortices started to form. To properly utilize an HPS-

CVD system, the inlet gas velocities need to be matched to susceptor rotational speeds to achieve optimal performance for different growth regimes. This is not thought to be limiting as precursor concentrations within the gas stream could be modified to counteract the velocity changes leading to comparable mass flow rates.

Stable laminar flow patterns were achieved in the third-generation design at 100 atm for nitrogen gas suggesting viability of this new HPS-CVD system. Additional, complementary studies are needed to specifically analyze thermal gradients within the system and associated mass transport and kinetics of chemical reactions.

4.4. Growth analysis

The investigated HPS-CVD reactor design is anticipated to provide enhanced growth rates compared to the super-atmospheric horizontal MOCVD reactor designed by Dr. Dietz's group [50]. Dietz's high-pressures CVD reactor design [10,50] showed a reduction in growth rate beyond growth pressures of 5 atm due to onset of turbulence within the chamber. This presumably led to a loss of source material via pre-reaction of the precursors in the gas phase. The HPS-CVD reactor addresses these shortcomings by physically separating the precursors thereby controlling flow pattern throughout the chamber. Precursor pre-mixing is thus primarily limited to the user-defined boundary layer and the time they reside within the boundary layer. Shorter residence time statistically leads to fewer pre-reactions of the precursors and hence source material loss.

Using information provided by CFD simulations for the third-generation design, it is possible to estimate achievable growth rates on a substrate within the HPS-CVD system. This analysis does not utilize specific mass transport modeling capabilities of COMSOL. Rather, it is based on the approach of determining the prevalent boundary layer thickness and resulting time required for gases to diffuse through the boundary layer to the surface of the substrate. Sufficient mixing in the boundary layer is presumed to occur based on simulations suggesting it can be considered to be similar to traditional MOCVD systems and growth processes are limited by mass transport.

Laminar flow patterns were achieved in the third-generation design at pressures up to 100 atm with well-defined boundary layers. The thickness of the boundary layer was calculated using CFD modeling results. While the boundary layer thickness is constant below the separation barriers, it increases within the chamber by up to 50% (from 0.1 to 0.15 in.). For species diffusion through the boundary layer, an average value of the boundary layer was applied (0.125 in.) as schematically presented in Fig. 11. Boundary layer thickness is primarily determined by the separation distance between the barrier and the susceptor and was found to only have a weak dependence on parameters such as inlet velocity, total system pressure, and rotation speed of the susceptor.

Using Fick's second law to determine the diffusion time for trimethylgallium (TMGa) [21] through a nitrogen boundary layer in the HPS-CVD operating at a 400 rpm rotational speed for the susceptor, it is found to be at least 5 times shorter than the time the precursor needs to travel to reach the substrate surface in Dietz's MOCVD reactor after it was introduced into the common gas stream. While Dietz's high-pressure CVD reactor design [10,51] used pulsed precursors injection to reduce the premixing of precursors, it didn't eliminate them as evidenced by continued reduction in growth rate as the reactor pressure increases. This is thought to be due to existing turbulence or vortices in the system which leads to mixing of precursors despite temporal separation in their introduction. Overall, it is anticipated that the proposed HPS-CVD system will have a higher concentration of precursors available to incorporate into the film due to reduced adduct formation and pre-reactions. As growth occurs in the mass transport limited regime, it is estimated that an increase in growth rate may occur by up to a factor of 5.

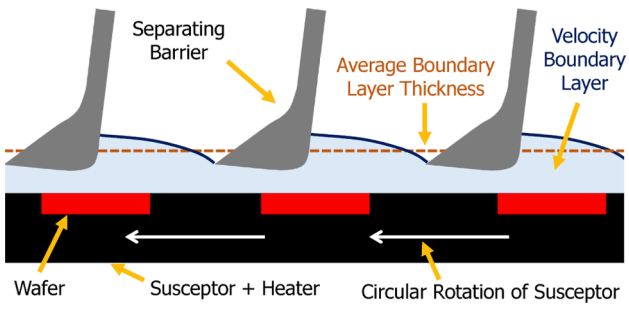

Fig. 11. Schematic cross-section view of the HPS-CVD reactor, which represents the boundary layer thickness where the heated wafer sequentially moves between the individual chambers via rotation of the susceptor.

To reduce precursor loss due to surface-related effects, including undesirable surface reactions or depositions, the HPS-CVD design significantly reduces exposed surface to the mixed precursor gases as compared to Dietz's MOCVD design. The exposed surface area reduction is estimated to be at least a factor of 4 for the current HPS-CVD design. While this reduction doesn't necessarily translate to 4-times increase in available precursor for growth (and hence growth rate), it is anticipated that an improvement in precursor availability of at least a factor of 2 is plausible.

Based on these factors, it is crudely and conservatively estimated that a growth rate enhancement of approximately 10 times is achievable compared to the existing state-of-the-art design by Dietz's group. This suggests growth rates up to 4 μm/hr are achievable in an HPS-CVD system operating at elevated pressures. This growth rate is comparable to existing atmospheric MOCVD reactors.

5. Summary

This paper applied CFD techniques to investigate the viability of a new vertical-type high pressure CVD reactor which is capable of growth at up to 100 atm system pressure for high quality growth of high-In content group III nitrides. The effects of rector design, chamber height, system pressure, inlet flow rate, and rotational speed were investigated. It was found that by reducing the height of the chamber, the flow instabilities reduced significantly due to the suppression of the thermal and mass transfer boundary layers caused by the geometry of the reduced space. In addition, modeling results demonstrated that nitrogen gas is more susceptible to formation of vortex patterns as compared to hydrogen. Analysis of streamlines suggests that matching of inlet velocity to rotational speed of the susceptor is necessary to optimize source gas coverage of the substrate. Although, stable laminar flow patterns were achieved in the third-generation design at 100 atm for nitrogen gas, complementary studies are needed to analyze thermal gradients within the system and associated mass transport and kinetics of chemical reactions.

Growth rates were estimated in a comparative fashion to an existing super-atmospheric system and a growth rate enhancement by up to a factor of 10 is determined to be plausible. This would lead to an HPS-CVD system with growth rates up to 4 μm/hr which is comparable to existing atmospheric MOCVD systems.

CRediT authorship contribution statement

Pedram Yousefian: Conceptualization, Methodology, Software, Validation, Formal analysis, Investigation, Data curation, Writing - original draft, Visualization. **Siddha Pimputkar:** Conceptualization, Methodology, Resources, Writing - review & editing, Supervision, Project administration, Funding acquisition.

Declaration of Competing Interest

The authors declare that they have no known competing financial interests or personal relationships that could have appeared to influence the work reported in this paper.

Acknowledgements

This work was supported by Lehigh University through new-faculty start-up funds and the National Science Foundation Major Research Instrumentation (NSF-MRI) under Grant No. 1745826.

References

[1] T.J. Flack, B.N. Pushpakaran, S.B. Bayne, GaN Technology for Power Electronic Applications: A Review, J. Electron. Mater. 45 (2016) 2673–2682, https://doi.org/10.1007/s11664-016-4435-3.
[2] Y. Kim, H.-B. Shin, W.-H. Lee, S.H. Jung, C.Z. Kim, H. Kim, Y.T. Lee, H.K. Kang, 1080 nm InGaAs laser power converters grown by MOCVD using InAlGaAs metamorphic buffer layers, Sol. Energy Mater. Sol. Cells. 200 (2019), 109984, https://doi.org/10.1016/j.solmat.2019.109984.
[3] J.B. MacChesney, P.M. Bridenbaugh, P.B. O'Connor, Thermal stability of indium nitride at elevated temperatures and nitrogen pressures, Mater. Res. Bull. 5 (1970) 783–791, https://doi.org/10.1016/0025-5408(70)90028-0.
[4] A. Yamamoto, K. Sugita, A. Hashimoto, Elucidation of factors obstructing quality improvement of MOVPE-grown InN, J. Cryst. Growth. 311 (2009) 4636–4640, https://doi.org/10.1016/j.jcrysgro.2009.08.027.
[5] L. Lymperakis, T. Schulz, C. Freysoldt, M. Anikeeva, Z. Chen, X. Zheng, B. Shen, C. Chèze, M. Siekacz, X.Q. Wang, M. Albrecht, J. Neugebauer, Elastically frustrated rehybridization: Origin of chemical order and compositional limits in InGaN quantum wells, Phys. Rev. Mater. 2 (2018), 011601, https://doi.org/10.1103/PhysRevMaterials.2.011601.
[6] S.V. Ivanov, T.V. Shubina, T.A. Komissarova, V.N. Jmerik, Metastable nature of InN and In-rich InGaN alloys, J. Cryst. Growth. 403 (2014) 83–89, https://doi.org/10.1016/j.jcrysgro.2014.06.019.
[7] D. Borovac, W. Sun, M.R. Peart, R. Song, J.J. Wierer, N. Tansu, Low background doping in AlInN grown on GaN via metalorganic vapor phase epitaxy, J. Cryst. Growth. 548 (2020), 125847, https://doi.org/10.1016/j.jcrysgro.2020.125847.
[8] M. Miyoshi, M. Yamanaka, T. Egawa, T. Takeuchi, Microstructure variation in thick AlInN films grown on c-plane GaN on sapphire by metalorganic chemical vapor deposition, J. Cryst. Growth. 506 (2019) 40–44, https://doi.org/10.1016/j.jcrysgro.2018.09.049.
[9] B.P. Burton, A. van de Walle, U. Kattner, First principles phase diagram calculations for the wurtzite-structure systems AlN–GaN, GaN–InN, and AlN–InN, J. Appl. Phys. 100 (2006), 113528, https://doi.org/10.1063/1.2372309.
[10] V.T. Woods, High pressure chemical vapor deposition: A novel approach for the growth of indium nitride, Georgia State University, 2006.
[11] N. Dietz, H. Born, M. Strassburg, V. Woods, Real-time optical monitoring of gas phase dynamics for the growth of InN at elevated pressures, MRS Proc. 798 (2003), https://doi.org/10.1557/PROC-798-Y10.45. Y10.45.
[12] N. Dietz, M. Alevli, H. Kang, M. Strassburg, V. Woods, I.T. Ferguson, C.E. Moore, B. H. Cardelino, The growth of InN and related alloys by high-pressure CVD, Proc. SPIE. 5912 (2005) 5912, https://doi.org/10.1117/12.616699.
[13] N. Dietz, High pressure chemical vapor deposition apparatuses, methods, and compositions produced therewith, 2013. http://portal.acm.org/citation.cfm?doid=634067.634234.
[14] M. Alevli, G. Durkaya, A. Weerasekara, A.G.U. Perera, N. Dietz, W. Fenwick, V. Woods, I. Ferguson, Characterization of InN layers grown by high-pressure chemical vapor deposition, Appl. Phys. Lett. 89 (2006) 1–4, https://doi.org/10.1063/1.2352797.
[15] M.K. Indika Senevirathna, S. Gamage, R. Atalay, A.R. Acharya, A.G. Unil Perera, N. Dietz, M. Buegler, A. Hoffmann, L. Su, A. Melton, I. Ferguson, Effect of reactor pressure on the electrical and structural properties of InN epilayers grown by high-pressure chemical vapor deposition, J. Vac. Sci. Technol. A Vacuum, Surfaces, Film. 30 (2012), 031511, https://doi.org/10.1116/1.4705727.
[16] L.J. Giling, Gas Flow Patterns in Horizontal Epitaxial Reactor Cells Observed by Interference Holography, J. Electrochem. Soc. 129 (1982) 634, https://doi.org/10.1149/1.2123939.
[17] R. Takahashi, Y. Koga, K. Sugawara, Gas Flow Pattern and Mass Transfer Analysis in a Horizontal Flow Reactor for Chemical Vapor Deposition, J. Electrochem. Soc. 119 (1972) 1406, https://doi.org/10.1149/1.2404006.
[18] C.-C. Wang, K.-C. Chen, C.-D. Tsai, J.-C. Chian, C.-L. Chao, Y.-J. Lin, C.-Y. Huang, Development of a novel gas spray module for MOCVD systems, 14th IFToMM World Congr. (2015) 80–83, https://doi.org/10.6567/IFToMM.14TH.WC.PS2.001.
[19] B. Mitrovic, A. Gurary, L. Kadinski, On the flow stability in vertical rotating disc MOCVD reactors under a wide range of process parameters, J. Cryst. Growth. 287 (2006) 656–663, https://doi.org/10.1016/j.jcrysgro.2005.10.131.
[20] S. Wong, Y. Jaluria, Numerical simulation of a practical chemical vapor deposition reactor, Numer. Heat Transf. Part A Appl. 70 (2016) 1057–1071, https://doi.org/10.1080/10407782.2016.1230421.
[21] R.L. Mahajan, Transport Phenomena in Chemical Vapor-Deposition Systems, Adv. Heat Transf. (1996) 339–425, https://doi.org/10.1016/S0065-2717(08)70143-6.
[22] E. Raj, Z. Lisik, P. Niedzielski, L. Ruta, M. Turczynski, X. Wang, A. Waag, Modelling of MOCVD Reactor: New 3D Approach, J. Phys. Conf. Ser. 494 (2014), 012019, https://doi.org/10.1088/1742-6596/494/1/012019.
[23] C.H. Lin, W.T. Cheng, J.H. Lee, Effect of embedding a porous medium on the deposition rate in a vertical rotating MOCVD reactor based on CFD modeling, Int. Commun. Heat Mass Transf. 36 (2009) 680–685, https://doi.org/10.1016/j.icheatmasstransfer.2009.03.019.
[24] Ł.J. Sytniewski, A.A. Lapkin, S. Stepanov, W.N. Wang, CFD optimisation of up-flow vertical HVPE reactor for GaN growth, J. Cryst. Growth. 310 (2008) 3358–3365, https://doi.org/10.1016/j.jcrysgro.2008.04.017.
[25] S. Harmand, J. Pellé, S. Poncet, I.V. Shevchuk, Review of fluid flow and convective heat transfer within rotating disk cavities with impinging jet, Int. J. Therm. Sci. 67 (2013) 1–30, https://doi.org/10.1016/j.ijthermalsci.2012.11.009.
[26] G.P. Gakis, E.D. Koronaki, A.G. Boudouvis, Numerical investigation of multiple stationary and time-periodic flow regimes in vertical rotating disc CVD reactors, J. Cryst. Growth. 432 (2015) 152–159, https://doi.org/10.1016/j.jcrysgro.2015.09.026.
[27] H.S. Fang, Y.Y. Pan, J.A. Wei, S. Liu, Z. Zhang, L.L. Zheng, Numerical Study and Optimization of GaN Thin-Film Growth by MOCVD Method, Heat Mass Transf. Under Extrem. Cond. Environ. Heat Transf. Comput. Heat Transf. Vis. Heat Transf. Heat Transf. Educ. Futur. Dir. Heat Transf. Nucl. Energy, Am. Soc. Mech. Eng. 4 1 8 (2013), https://doi.org/10.1115/HT2013-17598.
[28] S. Tabatabaei, Evaluation of fluid dynamic effect on thin film growth in a horizontal type meso-scale chemical vapor deposition reactor using computational fluid dynamics, University of Alabama, 2013.
[29] P. Kempisty, B. Łucznik, B. Pastuszka, I. Grzegory, M. Boćkowski, S. Krukowski, S. Porowski, CFD and reaction computational analysis of the growth of GaN by HVPE method, J. Cryst. Growth. 296 (2006) 31–42, https://doi.org/10.1016/j.jcrysgro.2006.08.008.
[30] G. Evans, R. Greif, Effects of boundary conditions on the flow and heat transfer in a rotating disk chemical vapor deposition reactor, Numer. Heat Transf. 12 (1987) 243–252, https://doi.org/10.1080/10407788708913584.
[31] C. Kleijn, Transport phenomena in chemical vapor deposition reactors, Delft University, 1991.
[32] C. Theodoropoulos, T.J. Mountziaris, H.K. Moffat, J. Han, Design of gas inlets for the growth of gallium nitride by metalorganic vapor phase epitaxy, J. Cryst. Growth. 217 (2000) 65–81, https://doi.org/10.1016/S0022-0248(00)00402-4.
[33] S.P. Vanka, G. Luo, N.G. Glumac, Parametric effects on thin film growth and uniformity in an atmospheric pressure impinging jet CVD reactor, J. Cryst. Growth. 267 (2004) 22–34, https://doi.org/10.1016/j.jcrysgro.2004.03.039.
[34] B. Mitrovic, A. Gurary, W. Quinn, Process conditions optimization for the maximum deposition rate and uniformity in vertical rotating disc MOCVD reactors based on CFD modeling, J. Cryst. Growth. 303 (2007) 323–329, https://doi.org/10.1016/j.jcrysgro.2006.11.247.
[35] C.R. Biber, C.A. Wang, S. Motakef, Flow regime map and deposition rate uniformity in vertical rotating-disk OMVPE reactors, J. Cryst. Growth. 123 (1992) 545–554, https://doi.org/10.1016/0022-0248(92)90616-Q.
[36] S. Patnaik, R.A. Brown, C.A. Wang, Hydrodynamic dispersion in rotating-disk omvpe reactors: Numerical simulation and experimental measurements, J. Cryst. Growth. 96 (1989) 153–174, https://doi.org/10.1016/0022-0248(89)90285-6.
[37] D.W. Weyburne, B.S. Ahern, Design and operating considerations for a water-cooled close-spaced reactant injector in a production scale MOCVD reactor, J. Cryst. Growth. 170 (1997) 77–82, https://doi.org/10.1016/S0022-0248(96)00617-3.
[38] T.G. Mihopoulos, S.G. Hummel, K.F. Jensen, Simulation of flow and growth phenomena in a close-spaced reactor, J. Cryst. Growth. 195 (1998) 725–732, https://doi.org/10.1016/S0022-0248(98)00648-4.
[39] D.I. Fotiadis, S. Kieda, K.F. Jensen, Transport phenomena in vertical reactors for metalorganic vapor phase epitaxy, J. Cryst. Growth. 102 (1990) 441–470, https://doi.org/10.1016/0022-0248(90)90403-8.
[40] V. Gupta, C. Theodoropoulos, J.D. Peck, T.J. Mountziaris, Optimal Design of Stagnation-Flow MOVPE Reactors with Axisymmetric Multi-Aperture Inlets, MRS Proc. 490 (1997) 161, https://doi.org/10.1557/PROC-490-161.
[41] D. Muñoz-Rojas, V.H. Nguyen, C. Masse de la Huerta, S. Aghazadehchors, C. Jiménez, D. Bellet, Spatial Atomic Layer Deposition (SALD), an emerging tool for energy materials, Application to new-generation photovoltaic devices and transparent conductive materials, Comptes Rendus Phys. 18 (2017) 391–400, https://doi.org/10.1016/j.crhy.2017.09.004.
[42] N. Memon, Y. Jaluria, Flow Structure and Heat Transfer in a Stagnation Flow CVD Reactor, J. Heat Transfer. 133 (2011), 082501, https://doi.org/10.1115/1.4003749.
[43] Y.-H. Liu, G.-J. Peng, W.-C. Lai, C.-Y. Huang, J.-H. Liang, Flow field investigation in a rotating disk chemical vapor deposition chamber with a perforated showerhead, Exp. Therm. Fluid Sci. 88 (2017) 389–399, https://doi.org/10.1016/j.expthermflusci.2017.06.018.
[44] S.Y. Karpov, Advances in the modeling of MOVPE processes, J. Cryst. Growth. 248 (2003) 1–7, https://doi.org/10.1016/S0022-0248(02)01838-9.
[45] COMSOL Multiphysics® V. 5.4, (n.d.). https://www.comsol.com/.
[46] SolidWorks, (n.d.).
[47] B. Mitrovic, A. Parekh, J. Ramer, V. Merai, E.A. Armour, L. Kadinski, A. Gurary, Reactor design optimization based on 3D modeling of nitrides deposition in MOCVD vertical rotating disc reactors, J. Cryst. Growth. 289 (2006) 708–714, https://doi.org/10.1016/j.jcrysgro.2005.12.107.
[48] C.F. Tseng, T.Y. Tsai, Y.H. Huang, M.T. Lee, R.H. Horng, Transport phenomena and the effects of reactor geometry for epitaxial GaN growth in a vertical MOCVD

reactor, J. Cryst. Growth. 432 (2015) 54–63, https://doi.org/10.1016/j.jcrysgro.2015.09.003.
[49] H. Van Santen, C.R. Kleijn, H.E.A. Van Den Akker, Symmetry breaking in a stagnation-flow CVD reactor, J. Cryst. Growth. 212 (2000) 311–323, https://doi.org/10.1016/S0022-0248(00)00034-8.
[50] V. Woods, N. Dietz, InN growth by high-pressures chemical vapor deposition: Real-time optical growth characterization, Mater. Sci. Eng. B Solid-State Mater. Adv. Technol. 127 (2006) 239–250, https://doi.org/10.1016/j.mseb.2005.10.032.
[51] N. Dietz, V. Woods, S.D. McCall, K.J. Bachmann, Real-Time Optical Monitoring Simulations of Gas Phase Kinetics in InN Vapor Phase Epitaxy at High Pressure, Microgravity Mater. Sci. Conf. 2003 (2002) 1662–1681.